



Simulation of Cylindrical Body Structure Subjected to Flow in Different Reynolds Number Regimes

Mohammed J. Mawat

Civil Engineering Department, University of Basra, Iraq.

ARTICLE INFO

Received: 20/10/2017

Accepted: 21/02/2018

Keywords

Computational Fluid Dynamic, Reynolds number, Vortex induced vibration, Von Karman street

ABSTRACT

A vacillating forces on the body are causes by The vortex shedding vacillate, and generating a cyclic variation in two directions, cross flow(CF), in same direction of flow and in-line(IL) with direction normal to flow. Determination of the force components, (CF) and (IL) directions is important when doing further Lock-in state. As a choice an alternative to response models the Computational Fluid Dynamics (CFD) simulations is presented and can be adopted for vortex induced vibration (VIV) analysis to conquer the restrictions of the status approach of practice engineering. To estimate the lift and drag coefficients the turbulent flow is simulated depending on shear stress transport(SST) of $k-\omega$ turbulence model with characteristics which utilized time dependent test (transient) using ANSYS FLUENT 16.1 and examined at various values of Reynolds number (30, 75, 200 and 1000) with uniform velocities of (0.06, 0.15, 0.4 and 2) m/s to overcome laminar, transport and turbulence regimes. At $Re < 40$ no lift force component will effect on the cylinder, then it clearly appears in the regime Re greater than 40.

محاكاة منشأ اسطواني الشكل معرض إلى جريان في أطوار مختلفة من رقم رينولدز

الخلاصة

تولد الدوامة المنفصلة قوى متذبذبة على الجسم وتجعله في حالة تأرجح باتجاهين. (الاتجاه العمودي على الخط المركزي للجسم والذي يكون باتجاه التيار(CF) و الاتجاه الموازي للخط المركزي (IL)). وبالتالي ينتج تغير دوري على مركبات هذه القوى المؤثرة على الجسم الاسطواني الشكل. لذلك من الضروري حساب مركبات القوى بالاتجاهين تجنباً لحدوث ظاهرة الرنين. تم عمل محاكاة لجريان المائع على جسم اسطواني الشكل لتمثيل الدوامات المتولدة ودراسة الاهتزاز الناتج منها بواسطة برنامج ANSYS FLUENT 16.1. حيث اعتمدت نظرية انتقال أجهاد القص ($SST/k-\omega$) لتمثيل الجريان المضطرب غير الثابت. ولمعرفة المراحل التي تتكون خلالها الدوامات تم اختبار سرعات مختلفة للمائع وبالتالي قيم مختلفة لرقم رينولدز لتشمل الجريان الصفائحي والانتقالي والمضطرب. حيث نلاحظ مركبة قوة الرفع غير موجودة عندما تكون قيمة رقم رينولدز اقل من 40، ولكنها تتولد وتتزايد عند زيادة رقم رينولدز لأكثر من 40.

الكلمات المفتاحية

ديناميكا الموائع الحسابية, رقم رينولدز, الدوامات المسببة للاهتزاز, نظرية فون كارمن

*Corresponding author:

E-mail addresses: mohammed.mawat@gmail.com

©2018 AL-Muthanna University. All rights reserved.

DOI:10.52113/3/eng/mjet/2018-06-01/45-51

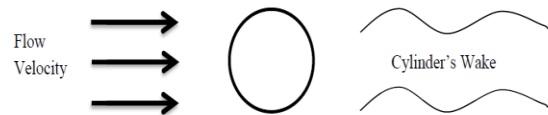


Figure 1: Representation of Von Karman street.

As a standard, 2D computational simulations are formed with fluent CFD to model flow over a cylinder at various Reynolds numbers. Reynolds Number (Re) is an important non dimensional number that is guess flow patterns, refers to the relevance among inertia force and the viscosity force and is classified commonly by 4 regimes which is subcritical, critical, supercritical and trans critical. The major regimes of interest for the entire range of Reynolds numbers are sketched in Fig. 2[6]. It is well known that the phenomenon of vortex-induced vibration (VIV) at a subcritical Reynolds number, which is less than 47[7].

Introduction

During the exposure of a body, especially the bluff body as cylinder on flow pattern the vortex shedding is generated behind the cylinder, thus the body will be in vibrate because of irregular pressure distribution when low pressure at the downstream zone. This is currently known as a Von Karman vortex street[1]. Theodore Von Karman was a pioneer in this field. A good representation of Von Karman street is shown in figure 1. The resonance, it is one of possible reasons of structure's failure, occurs when the vortex's frequency meets with natural frequency of the body. The earliest studies on vortex shedding and vortex induced vibration (VIV) was related to experiments on cylinders submerged in water as a pipelines of oil and gas export through sea water. It is found from those studies that need more attention and work to understanding effect of fluid and structure proprieties[2,3]. B.N. Rajani, et al (2009)[4] focused on the study 2D and 3Dflow past a cylindrical body. Computations have been carried out for various Reynolds numbers covering different laminar flow using The implicit finite volume solver (RANS3D) code. Pietro Catalano et al (2003) [5], examined complex turbulent flows for high Reynolds number in the supercritical regime by using large-eddy simulation (LES) and they compared with Reynolds-averaged Navier–Stokes algorithmic (RANS) solutions. As appear from the results, the LES solutions were significantly more accurate than the RANS results.

Fluid Theory

Many processes(approximately and experimentally) have been considered in the analysis of uniform flow over a 2-Dimensional cylindrical body. Development of vortices at the rear the cylinder's wake is one of the fundamental problems study, that is clarified in Fig. 1.

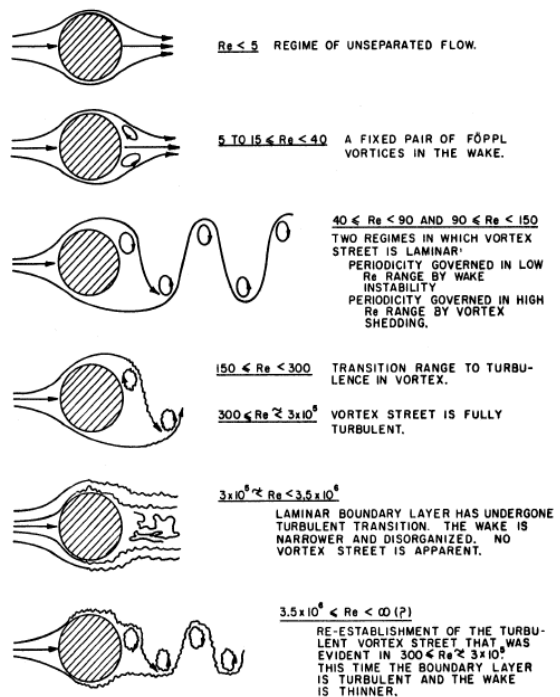


Figure 2: Vortex shedding pattern for different Reynolds number [6].

At low Reynolds number, less than 40, just drag force component (F_d) exerted strenuously on the cylinder in same direction of flow motion due to all flows in that regime are proportioned according to the flow direction. When Re greater than 40 another force component normal to the flow direction (lift force, F_l) is created because effect of a Vortex sensitivity and shedding[6], see Fig. 3. Drag coefficient, Cd is given by[8];

$$cd = \frac{2F_d}{\rho DU^2} \quad (1)$$

Where;

F_d is the summation of the pressure force, D is the diameter, ρ is the fluid density and U is the flow velocity. Lift coefficient, C_l is calculated same way of C_d except that the pressure force will be vertical and given by[8];

$$cl = \frac{2F_l}{\rho DU^2} \quad (2)$$

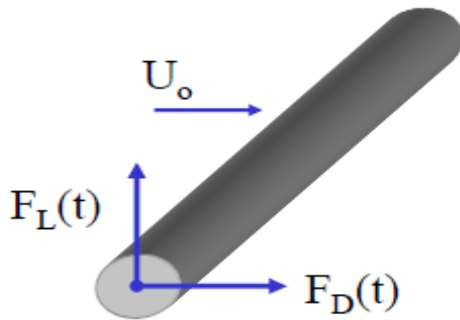


Figure 3: Force components that acts on a cylinder

Modeling Procedures

Fig. 4 shows the Sketch of Geometry view for 2-Dimensional fluid domain created in ANSYS FLUENT. Since ANSYS FLUENT is a state-of-the-art computer program for modeling fluid flow, heat transfer, and chemical reactions in complex geometries. The number of cells used to mesh the environment directly affects the accuracy and length of time of the solution[9]. So the height of the domain is 0.1m and the length 0.25m. The circle has a diameter of d is 0.01m and the distance from lower left corner to center of the circle is 0.05m in two directions. Therefore no thickness to fluid domain. The fluid domain is meshed with 5916 cell, since the length of cell is equal to 0.003m, and generated as shown in Fig. 5.

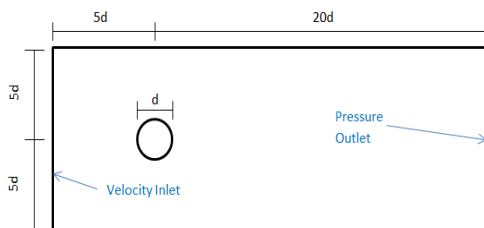


Figure 4: the Sketch of Geometry view for fluid domain

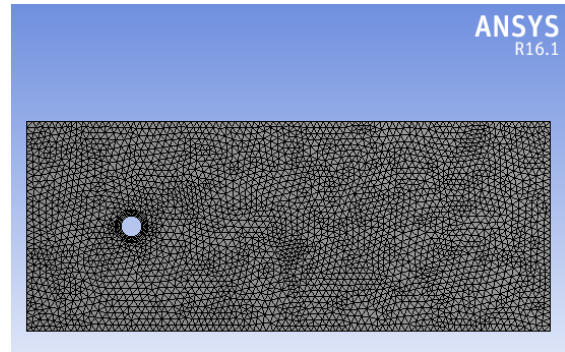


Figure 5: Triangular Mesh view for fluid domain

Physics parameters of flow material enabled in this simulation included:

- Flow material is water
- Flow material is incompressible liquid has constant density.
- Time model is Implicit unsteady.

This choice is used to observe the vortex shedding behind the cylinder, for this is a time-dependent problem (unsteady) and the governing equations used in this analysis are too complex to solve by explicit approach. In this method a certain convergence is achieved by using inner iterations. After each cycle of inner iteration, The time step going to update.

- Solver algorithm is simple
- Convection scheme is second order upwind
- Temporal discretization is second order.
- Viscous regime is laminar for $Re = 30$ and 75 and turbulence for $Re = 200$ and 1000 .

The parameters used for the main variables are listed in Table 1.

Table 1 :Physics Values and Parameters for simulation.

Density	1 kg/m ³
Dynamic Viscosity	2×10^{-5} Pa*s
Diameter	0.01m
Inlet Velocity(four cases)	(0.06, 0.15, 0.4 and 2)m/s
Time step	0.02s
Temporal Discretization	2nd-order
Base Size of Mesh	0.003m
Maximum Inner Iterations	25
Maximum Flow Time	8s

Boundary condition of model geometry shown in figure 4 is illustrated in table 2 for all simulations cases. The flow domain is treated as 2-Dimensional canal where the inlet is positioned at the left side while the outlet at the right. The lower and upper edges are walls and the surfaces are a symmetry surface.

Results and discussion

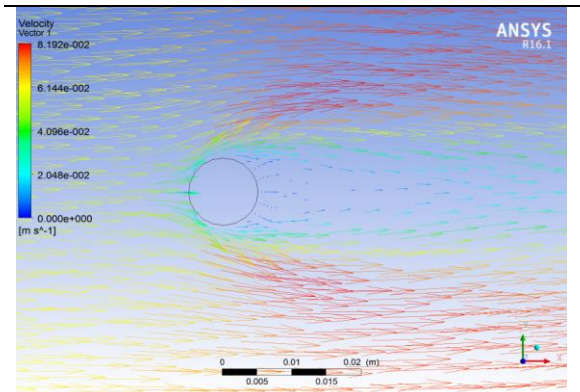
Four simulation cases for fluid domain is created at four different Reynolds number values according to magnitude of flow velocity. The velocity vector of surface body of first case at Reynolds number equals to 30 is plotted in Fig. 6-a. This figure shows good association between the results from FLUENT and those described in Fig. 2, where a pair of vortices in the wake clearly fixed. Second simulation was run with the Reynolds number updated to 75. To do that, the inlet velocity was increased from 0.06m/s to 0.15m/s. The FLUENT simulation properly displayed the von Karman Street behind the cylinder when Reynolds number equals 75. See Fig. 6-b.

The earlier cases(first and second) are presented laminar regime of flow and to discuss the transition and turbulence flow the Reynolds number will be increased to 200 and 1000 respectively. FLUENT 16.1 allows viscous turbulence modeling with the Spalart-Allmaras Turbulence model, the K- Omega Turbulence model, and the K- Epsilon Turbulence model. K-Omega Turbulence model of (SST) formulation was selected because of it is more accurate modeling because of limitations of the other models[10]. The FLUENT simulation as shown in Fig. 6-c precisely describes the von Karman Street behind the cylinder at a Reynolds number of 200 when compared to Fig. 2

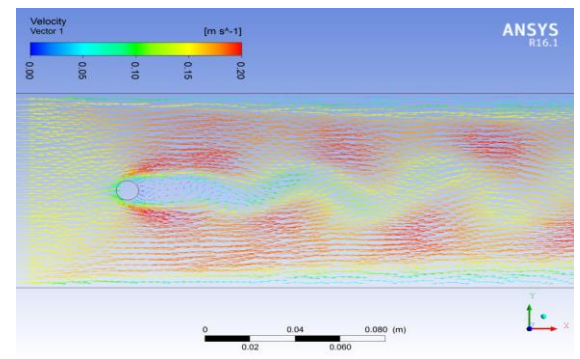
. A final simulation was run with the Reynolds number increased to 1000 by increase inlet velocity to 2m/s and use time step (0.005s) instead of (0.02s) to achieve more accurate results at higher values of Reynolds number. Fig. 6-d illustrate this results of Re =1000. From Fig. 7 it can be noted that the wake will become turbulent and narrower when the Reynolds number is increased.

Table 2. Boundary Conditions for fluid domain

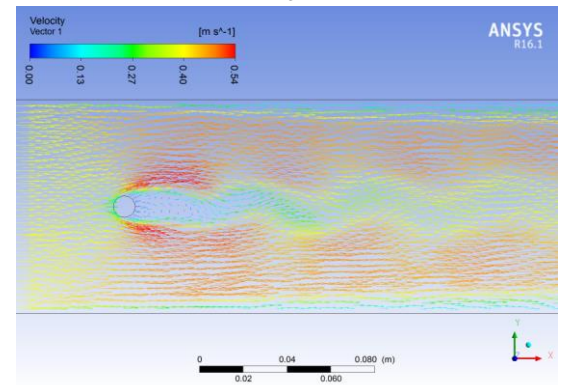
Inlet	Velocity inlet
Outlet	Pressure outlet
Upper edge	No slip-wall
Lower edge	No slip-wall
Cylinder	No slip-wall
Symmetry	Symmetry plane

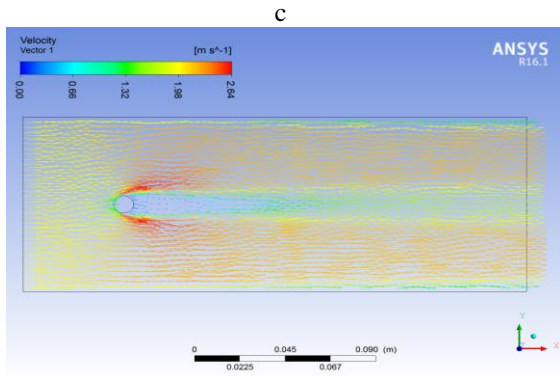


a



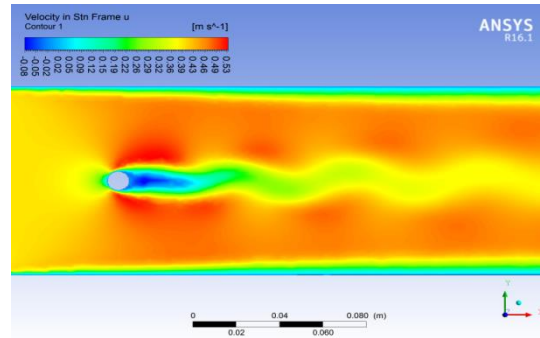
b



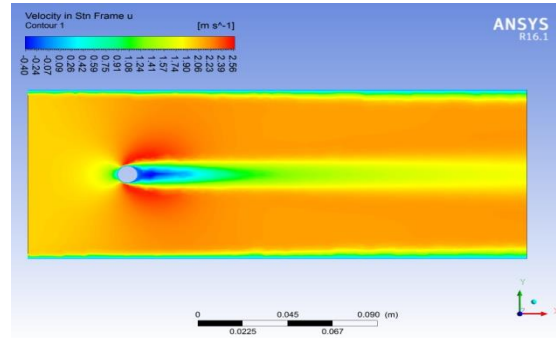


d

Figure 6: Velocity Vector view for various Reynolds numbers. (a) 30, (b) 75, (c) 200, and (d) 1000.

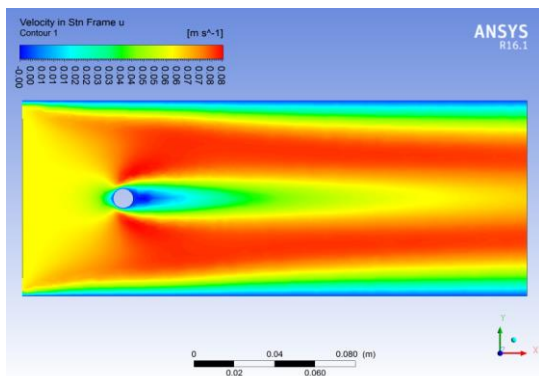


c

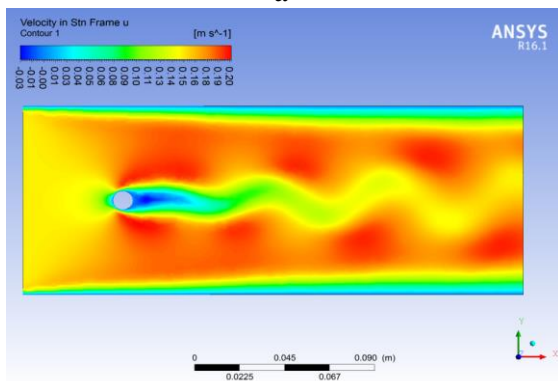


d

Figure 7: Velocity Contour view at various Reynolds numbers. (a) 30, (b) 75, (c) 200, and (d) 1000.

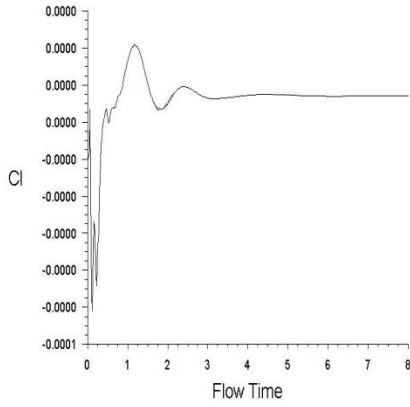


a



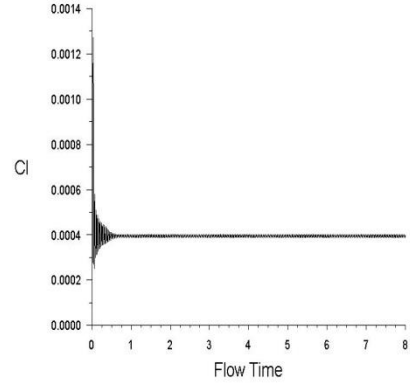
b

The lift and drag coefficients at different Re are presented in Fig. 8 and Fig. 9 respectively. As Re increases, the fluid system becomes more unstable and the disturbance grows faster, and the value of drag coefficient will be decrease while obviously development in value of lift coefficient is take place through the flow time. At Re=40, Fig. 8-a, the peak value of C_l is close to zero no lift force component will effects on the cylinder because the streams are symmetrical with respect to the direction of flow, then it clearly appears in the regime Re=75, Fig. 8-b, where value of C_l is observed to be growing at a very fast rate with time indicating the unsteady state of the wake. It can be noted that in unambiguous matter at Re=200, Fig. 8-c. A shorter wavelength with low alignment Of the wake give rise to constant value of C_l at Re=1000 as shown in Fig. 8-d.



cl-1 Convergence History (Time=8.0000e+00) ANSYS Fluent Release 16.1 (2d, dp, pbns, lam, transient) Jun 24, 2017

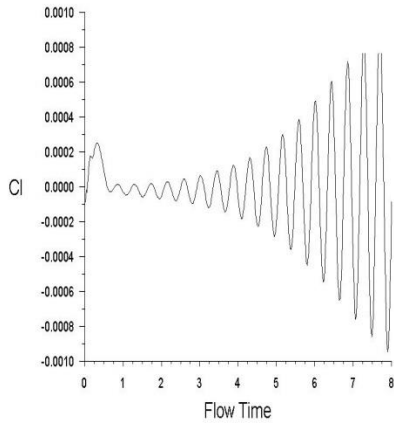
a



cl-1 Convergence History (Time=8.0000e+00) ANSYS Fluent Release 16.1 (2d, dp, pbns, sstk, transient) Jun 25, 2017

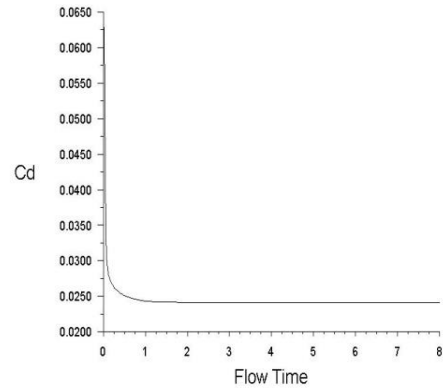
d

Figure 8: Reynolds numbers. (a) 30, (b) 75, (c) 200, and (d) 1000.



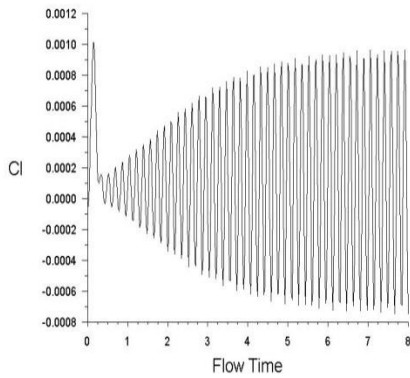
cl-1 Convergence History (Time=8.0000e+00) ANSYS Fluent Release 16.1 (2d, dp, pbns, lam, transient) Jun 24, 2017

b



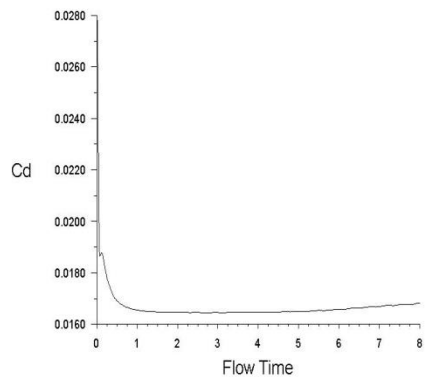
cd-1 Convergence History (Time=8.0000e+00) ANSYS Fluent Release 16.1 (2d, dp, pbns, lam, transient) Jun 24, 2017

a



cl-1 Convergence History (Time=8.0000e+00) ANSYS Fluent Release 16.1 (2d, dp, pbns, sstk, transient) Jun 24, 2017

c



cd-1 Convergence History (Time=8.0000e+00) ANSYS Fluent Release 16.1 (2d, dp, pbns, lam, transient) Jun 24, 2017

b

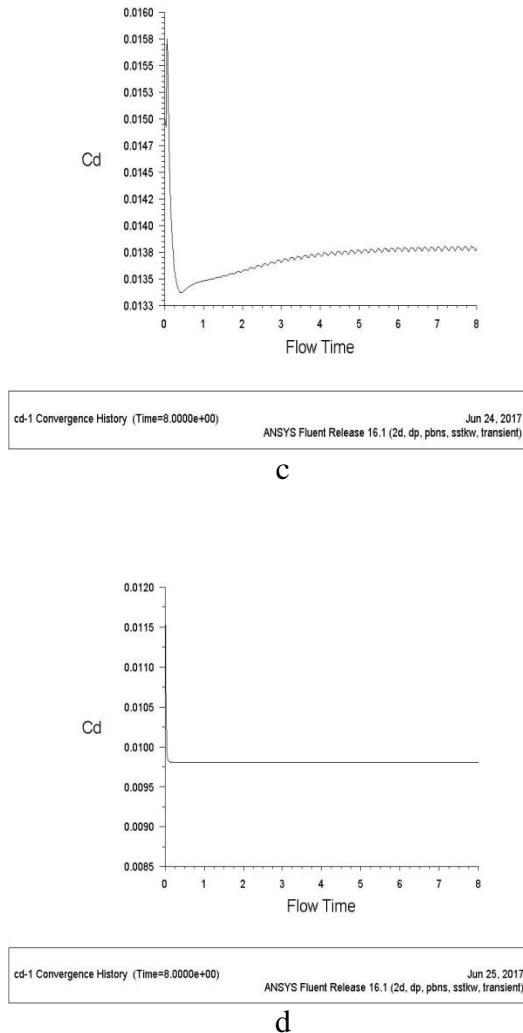


Figure 9: Temporal Drag coefficient response at various Reynolds numbers. (a) 30, (b) 75, (c) 200, and (d) 1000.

Conclusion

The objective of this study is to understand when the von Karman vortex street is shedding, and effects of this vortex on structure subjected to flow. Flows with various Reynolds number must be estimated to obtain a more obvious Scene of the method. when Re is smaller than 40, the vortex shedding mode lightly appears.. When $Re > 40$, The pair of vortices, which is behind to the cylinder surfaces develops and distinct, and continues to move back from the cylinder as the flow develops to the transition regime ($Re = 200$). The magnitude of this vortex pair increases while the wake vortex magnitude decreases when a comparison between flow patterns of $Re = 1000$ with the flow patterns of $Re = 200$. By observing these von Karman modes, it is obviously that the force component normal to flow direction is induced, where the pressure distributions on the upper and lower cylinder

surfaces are different. the value of drag coefficient will be decrease while obviously development in value of lift coefficient is take place through the flow time.

References

1. Gustafsson, A, 2012, "Analysis of Vortex-Induced Vibrations of Risers", Master's Thesis in Applied Mechanics, Department of Applied Mechanics, Division of Material and Computational Mechanics Chalmers, University of Technology Gothenburg, Sweden.
2. Roshko, A, 1954, " On The Development Of Turbulent Wakes From Vortex Streets", California Institute of Technology, USA.
3. Roshko, A, 1960," Experiments on the flow past a circular cylinder at very high Reynolds number", California Institute of Technology, USA.
4. Rajani, B, N , Kandasamy , A, Majumdar, S, 2009, " Numerical simulation of laminar flow past a circular cylinder.", Applied Mathematical Modelling 33,pp. 1228–1247.
5. Catalano, P, Wang, M , Iaccarino, G, Moin, P, 2003 "Numerical simulation of the flow around a circular cylinder at high Reynolds numbers." , International Journal of Heat and Fluid Flow Vol. 24,pp.463–469.
6. Lienhard, J, H, 1966, "Synopsis of Lift, Drag and Vortex Frequency Data For Rigid circular Cylinders", Technical Extension Service, Bulletin 300, College Engineering, Washington State University.
7. Jiaqing K, Weiwei Z, Yilang L, Xintao L, 2017,duced vibrations". American Institute of Physics,Vol.29,pp. 041701.
8. Fesal, S, N, 2015, "Simulation of Vortex Induced Vibration of a Bluff Body structure", A thesis submitted in fulfillment of the requirement for the award of the master of Mechanical Engineering, Universiti Tun Hussein Onn Malaysia.
9. Fluent R 16.1 Help.
10. Matsubara, C, Tim, K, Wu, H, 2013, " Comparison of the Effects of $k-\epsilon$, $k-\omega$, and Zero Equation Models on Characterization of Turbulent Permeability of Porous Media", Journal of Water Resource and Hydraulic Engineering, Vol. 2 No. 2, PP. 43-50.